An EPR/ENDOR investigation of a $[ZrPO_4]^0$ centre in x-irradiated zircon: the Zr(α) centre

2000 J. Phys.: Condens. Matter 12 1421

(http://iopscience.iop.org/0953-8984/12/7/323)

J. Phys.: Condens. Matter **12** (2000) 1421–1430. Printed in the UK PII: S0953-8984(00)07687-6

An EPR/ENDOR investigation of a $[ZrPO_4]^0$ centre in x-irradiated zircon: the Zr(α) centre

R F C Claridge†, W C Tennant†, C J Walsby†, S Schweizer‡ and J-M Spaeth‡

† Chemistry Department, University of Canterbury, Private Bag 4800, Christchurch, New Zealand

‡ Fachbereich Physik, Universität Paderborn, D33100 Paderborn, Germany

Received 10 September 1999

Abstract. The Zr(α) centre is the most prominent centre observed after low temperature x-irradiation of zirconium silicate (zircon). The centre has been identified as due to an electron trap in the form of a Zr^{3+} ion in the zircon lattice with the centre being stabilized by interaction with a 100% abundant $I = 1/2$ ion. Previous reports have discussed the Zr(α) centre in terms of an $^{89}Y^{3+}$ ($I = 1/2$) ion in a neighbouring Zr^{4+} site. Using both EPR and ENDOR it has now been possible to show unequivocally that the $I = 1/2$ nuclear interaction is due to the presence of a ^{31}P ion. Detailed analysis of the g and hyperfine matrices for ^{91}Zr, ^{31}P and ^{29}Si is used to develop a model of the centre as an electron trapped on zirconium as a Zr^{3+} ion with a P^{5+} ion in the nearest Si^{4+} site on the mirror plane. The defect is now best described as a $[ZrPO_4]^0$ centre.

1. Introduction

Zirconium silicate (zircon) is an interesting crystalline system in that it is intermediate between purely ionic crystals such as alkali halides and molecular crystals such as silicon dioxide (quartz) where covalent bonding prevails. In zircon, the cation Zr^{4+} is ionically 'bonded' to the covalently bonded SiO_4^{4-} negative units. In the tetragonal crystal (space group $I4_1/amd$) each Zr^{4+} ion is surrounded by eight oxygens of the SiO_4^{4+} units in the form of two interlocking distorted tetrahedra [1]. Each of the Zr^{4+} and Si^{4+} ions has dodecahedral, $\bar{4}2m$ (D_{2d}), point group symmetry.

Our interest in zircon arose in the first instance from the quality of the EPR information obtained for α-quartz and the possibility of extending this to other crystalline materials of technological interest. There is a keen interest in zircon as a 'high tech' material because of its high refractive index, its hardness and resistance to chemical attack. High purity synthetic zircon may be used in laser components, in which case it is important to be aware of the impurities, often at trace levels, which may be associated with unpaired electrons, and their consequent amenability to study by EPR.

Irradiation of natural zircons with x-rays at low temperature creates a number of thermally unstable defect centres. Solntsev and Shcherbakova [2] made the initial report on the EPR of zirconium based electron trap centres in natural zircon. They described three distinct d^1 Zr^{3+} centres formed by electron capture by Zr^{4+}. The centres were labelled Zr(α), Zr(β) and Zr(γ), the differences between the centres being attributed to the position of the Zr^{3+} in the crystal lattice. The Zr(α) centre was initially described as having $2/m$ point group symmetry [2], being lowered from that of the Zr^{4+} lattice site ($\bar{4}2m$) by the presence of an alkali metal ion. The Zr(β) centre also had lowered symmetry which was attributed to a neighbouring oxygen

0953-8984/00/071421+10$30.00

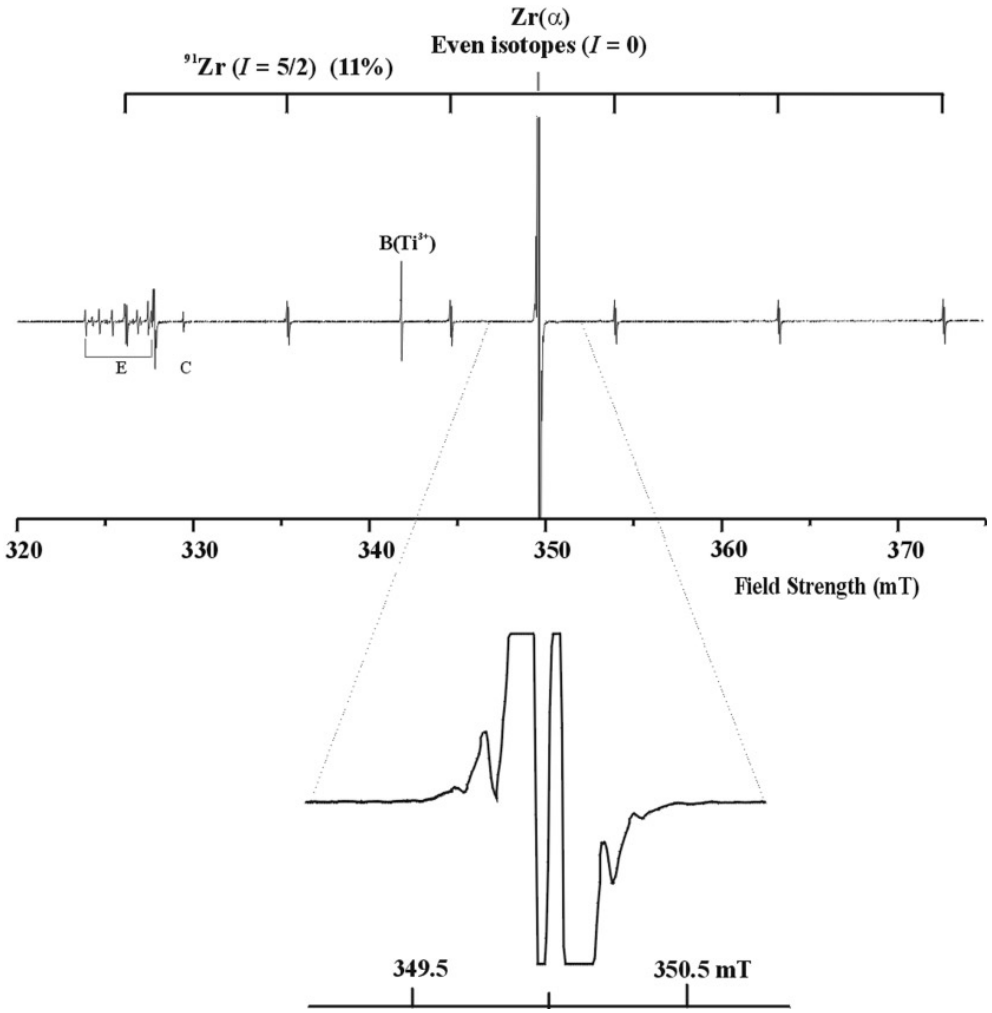

Figure 1. X-band spectrum ($\nu = 9.363$ GHz) of the Zr(α) centre in zircon at 15 K, $\boldsymbol{B} \parallel c$. See text for description of the labels. The expanded region shows the structure of the central line.

vacancy. From an analysis of the hyperfine structure on the Zr(γ) centre it was concluded that there was interaction with two 100% abundant $I = 1/2$ nuclei in neighbouring lattice sites. ^{89}Y was suggested as the most likely nucleus.

A more detailed study of undoped synthetic zircon crystals [3] showed that a centre corresponding to the Zr(α) centre of Solntsev and Shcherbakova was the most prominent electron centre formed in low temperature irradiation with x-rays. The Zr(β) and Zr(γ) centres are not present in any significant amount. No evidence for hyperfine interaction with a neighbouring alkali metal atom was found, nor indeed for the presence of any interstitial compensating ions. However, the narrow line width of the experiment revealed a clear doublet splitting discernible at most orientations. This was attributed to superhyperfine (shf) interaction with a single nucleus of 100% abundance and $I = 1/2$ which was presumed to be ^{89}Y on the basis that yttrium occurs naturally with zirconium in nature.

From the analysis of the Zr g and hyperfine matrices [3] it was concluded that the centre had $\bar{1}$ symmetry. While the g and ^{91}Zr hf matrices were well determined, the superhyperfine

matrix for the ^{89}Y could not be refined satisfactorily within the error of the experiment. With the development of new versions of EPRNMR [4] which are able to calculate transition intensities correctly it became evident that the doublet splitting could not be due to ^{89}Y. Examination of structural models showed that it was difficult to reconcile the symmetry of the defect centre with a sensible placement of the Y^{3+}. Small lines flanking the doublets, previously assigned to superhyperfine interactions with nearby ^{29}Si ions, varied in intensity more than might be expected with rotation of the magnetic field away from the *c*-axis. We set out to refine the so-called ^{89}Y matrices and to determine the ^{29}Si superhyperfine matrices to obtain a more detailed understanding of the Zr(α) centre.

We now present new EPR data which shows that the Zr(α) centre is an electron trapped on a Zr^{4+} ion to form a d^1 Zr^{3+} ion stabilized by a phosphorus ion in the neighbouring Si^{4+} site. ENDOR experiments give unequivocal proof of the presence of phosphorus and provide both ^{31}P and reasonable ^{29}Si superhyperfine matrices.

2. Experiment

Zircon crystals were grown from molten Li_2MoO_4–MoO_3 as described by Chase and Osmer [5]. The large crystal used in most of this work was obtained from Aerospace Corporation and was cut to a regular parallelepiped ($5.5\times3.5\times2.0\,mm^3$) with the rectangular faces parallel to the crystallographic axes. Smaller crystals grown in our own laboratory had well developed faces parallel to the *ac*- and *bc*-planes which allowed for precise mounting. Details of the crystal mounting, irradiation procedure and transfer to the EPR spectrometer at low temperature have been described previously [3]. The EPR measurements were performed on a modified Varian E12 X-band spectrometer at ~15 K using a closed cycle liquid helium refrigeration system at the University of Canterbury. Data were collected in two separate planes with the axis of rotation perpendicular to the static magnetic field: (a) the *bc*-plane, where the axis of rotation was the *a*-axis; (b) the 'magic angle' plane. In this case the axis of rotation was perpendicular to the *c*-axis and at an angle of 35.26° to the *a*-axis. Further measurements between 4.2 K and room temperature were made in a custom-built, computer-controlled X-band EPR/ENDOR spectrometer at the University of Paderborn using a variable temperature cryostat.

3. Results

3.1. EPR experiments

The EPR spectrum with $\boldsymbol{B} \parallel \boldsymbol{c}$ of zircon at ~15 K, following irradiation with x-rays at 77 K, is as shown in figure 1. The crystal alignment is, as described in [3], very precisely obtained from the observed degeneracies in the two planes of measurement. In the *bc*-plane two sites are always degenerate; three sites are observed in a general orientation collapsing two sites with $\boldsymbol{B} \parallel \boldsymbol{b}$ and to a single site with $\boldsymbol{B} \parallel \boldsymbol{c}$. In the 'magic angle' plane the four species in a general orientation collapse to one with $\boldsymbol{B} \parallel \boldsymbol{c}$. The spectrum of the Zr(α) centre with $\boldsymbol{B} \parallel \boldsymbol{c}$ consists of a strong central line arising from the even isotopes of zirconium (^{90}Zr (51.5%), ^{92}Zr (17.1%), ^{94}Zr (17.4%) and ^{96}Zr (2.8%)) surrounded by six hyperfine satellite lines due to the ^{91}Zr nucleus ($I = 5/2$, 11.2% abundance). Other centres, labelled B(Ti), E and C, are marked on this spectrum for reference. The B(Ti) is a Ti^{3+} centre [6, 7]. The E centre, $[AlO_4]^0$, is an oxygen hole centre associated with an Al^{3+} ion [8]. The C centre is an oxygen hole associated with a Zr^{4+} vacancy [9]. The expanded portion of figure 1 shows the central line of the Zr(α) spectrum under high resolution. The central line is now seen as a doublet with the splitting due to the 100% $I = 1/2$ nucleus with 'outrider' lines previously attributed to superhyperfine

Table 1. EPR spin Hamiltonian (SH) parameters for the Zr(α) centre[a–c]. Data from bc-plane and 'magic angle' plane.

	Matrix Y			k	Principal value Y_k	Principal direction[d] θ_k (°)	ϕ_k (°)
	1.924 18(1)	0	−0.005 610(5)	1	1.933 53(1)	90	90
$\boldsymbol{g}$		1.933 53(1)	0	2	1.924 95(1)	82.24(0)	0
			1.883 807(4)	3	1.883 043(4)	172.24(0)	0
Zirconium ^{91}Zr ($I = 5/2$) hyperfine interaction							
	4.890(1)	0	0.0629(6)	1	8.783 1(5)	179.07(1)	0
$\boldsymbol{A}/g_e\beta_e$		4.803(1)	0	2	4.888(1)	89.07(1)	0
(mT)			8.7821(5)	3	4.803(1)	90	90
	0.041(1)	0	0.0038(11)	1	0.079(1)	90	90
$\boldsymbol{P}/g_e\beta_e$		0.079(1)	0	2	0.041(1)	88.6(4)	0
(mT)			−0.1203(7)	3	−0.120 4(7)	178.6(4)	0
Phosphorus ^{31}P ($I = 1/2$) superhyperfine interaction							
	0.028(3)	0	0.024(2)	1	0.079(2)	155(6)	180
$\boldsymbol{A}/g_e\beta_e$		−0.207(3)	0	2	0.017(3)	115(6)	0
(mT)			0.068(1)	3	−0.207(3)	90	90

[a] Total number of data points = 1040.
[b] 619 unit weighted data points, RMSD = 0.017 mT.
[c] Error estimates in parentheses.
[d] Angle θ measured from c-axis and ϕ measured anticlockwise from a-axis.

splitting from neighbouring ^{29}Si ions. When the magnetic field was rotated away from the c-axis, the intensity and position of these 'outrider' lines varied more than could be expected if they arose solely from ^{29}Si ($I = 1/2$, 4.67% abundance) superhyperfine interaction. As discussed later, these lines are shown to be due to the 'spin flips' of ^{31}P. Some lines due to ^{29}Si are also identified. In a general direction in plane (b), the 'magic angle' plane, spectra from four distinct symmetry related sites are evident (see figure 2(b)).

The appropriate spin Hamiltonian (SH) for the analysis is

$$H_s = \beta_e \boldsymbol{S} \cdot \boldsymbol{g}_i \cdot \boldsymbol{B} + \sum_j \{\boldsymbol{S} \cdot (\boldsymbol{A}_j)_i \cdot \boldsymbol{I}_j - \beta_N \boldsymbol{I}_j \cdot (\boldsymbol{g}_{N_j})_i \cdot \boldsymbol{B} + \boldsymbol{I}_j \cdot (\boldsymbol{P}_j)_i \cdot \boldsymbol{I}_j\}. \tag{1}$$

The terms in the SH have their normal meanings. The subscript i (= 1–4) refers to the four symmetry related species. The subscript $j = 1$ refers to the ^{91}Zr nucleus and $j = 2$ to the $I = 1/2$ (100% abundance) nucleus. The ^{29}Si hyperfine interactions were not included in the analysis (however see later ENDOR analysis). Approximate fittings for $\boldsymbol{g}$ and $\boldsymbol{A}$ (^{91}Zr) were obtained by using $\boldsymbol{g}_N(^{91}\text{Zr}) = -0.521\,445\,\boldsymbol{U}$ ($\boldsymbol{U} = 3 \times 3$ unit matrix) and taking the average of the doublet splitting. Repeated measurements to ensure precise crystal orientation showed the site symmetry was $m(C_s)$ rather than $\bar{1}$ as stated earlier [3].

Attempts to fit the complete data set using the program EPRNMR [4] assuming that the second nucleus ($I = 1/2$) was ^{89}Y with $\boldsymbol{g}_N(^{89}\text{Y}) = -0.274\,855\,\boldsymbol{U}$ were unsatisfactory. A fit could be obtained, but the predicted intensities did not match the experimental spectra. At many orientations EPRNMR predicted four lines of almost equal intensity whereas never more than two intense transitions were observed in any orientation. This situation arises when the nuclear Zeeman term is of the same magnitude as the hyperfine term [10]. Eliminating ^{89}Y, the number of possible nuclei with $I = 1/2$, and 100% abundance is strictly limited, especially when it is required that magnitude of the $\boldsymbol{g}_N$ must be greater than that for ^{89}Y. The most likely candidate was ^{31}P with $\boldsymbol{g}_N = 2.263\,20\,\boldsymbol{U}$ and which could enter the zircon lattice as P^{5+} in an Si^{4+} site. There are several reports of the formation of mixed crystals between zircon and the

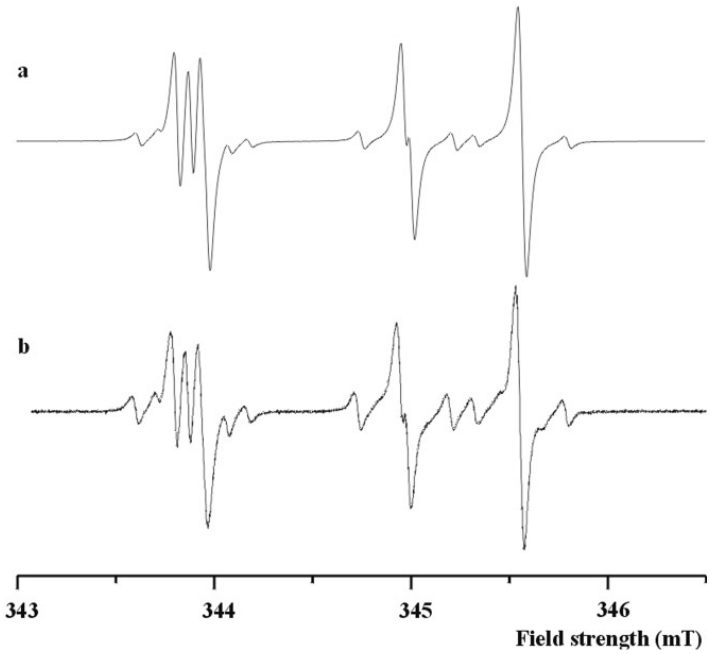

Figure 2. Comparison of (a) simulated spectrum and (b) measured spectrum due to the Zr ($I = 0$) isotopes using matrices in table 1. Crystal orientation: $\theta = 50.85^\circ$, $\phi = 35.25^\circ$, $\nu = 9.217$ GHz.

isomorphous mineral xenotime, YPO_4, [11]. Yttrium substitution into zircon has long been considered a very likely possibility. The presence of phosphorus in zircon however does not seem to be well documented [12]. In the present situation when the phosphorus g_N value was entered into the fitting routine an excellent fit was obtained.

Confirmation from EPR data that phosphorus was present came from the correct prediction of the positions of the 'spin flip' ($\Delta M_I = \pm 1$, $\Delta M_S = \pm 1$) transitions which appear as outriders on the main transitions. The separation of the transitions from the main transition is given by $\pm(g_N\beta_N/g_e\beta_e)B$. These lines had previously been attributed to ^{29}Si. Including data for these spin flip transitions in the fitting resulted in a decrease in the root-mean-squared deviation (RMSD) of the fitted lines. The results of the fitting are given in table 1. The data in table 1 result from a simultaneous fitting of a total of 1040 experimental points from the two planes—689 from the 'magic angle' plane and 351 from the *bc*-plane. Of the 1040 points 619 were given unit weighting: 430 and 189 from the 'magic angle' and *bc*-planes respectively. The overall RMSD was 0.017 mT, about half the peak-to-peak linewidth. When the data from the two planes was analysed separately the fit was better with the RMSD values of 0.011 and 0.009 mT respectively. The lower degree of fit (higher RMSD) for the combined data set results from a combination of factors including a slight field shift between the two mountings and slight misalignments of the crystal. The correctness of the assignment of the second nucleus to ^{31}P is shown in figure 2 where an experimental spectrum in an arbitrary direction, figure 2(b), whose data were not used in the fitting, is compared to the simulated spectrum, figure 2(a), generated using the matrices of table 1.

3.2. ENDOR experiments

The ENDOR spectrum between 0.5 and 10 MHz obtained while partially saturating the lower of the two lines of the central doublet ($I(^{91}\mathrm{Zr}) = 0$) of the Zr(α) centre with $\boldsymbol{B} \parallel \boldsymbol{c}$ is shown in

Table 2. ENDOR spin-Hamiltonian (SH) parameters for the Zr(α) centre[a].

	Matrix Y			k	Principal value Y_k	Principal direction[b] θ_k (°)	ϕ_k (°)
Phosphorus ^{31}P ($I = 1/2$) hyperfine interaction[c]							
$\boldsymbol{A}/g_e\beta_e$	0.0321(5)	0	0.0249(5)	1	−0.2124(5)	90	90
(mT)		−0.2123(5)	0	2	0.0803(5)	152.6(4)	180
			0.0674(5)	3	0.0193(5)	117.3(4)	0
Silicon ^{29}Si ($I = 1/2$) hyperfine interaction[d]							
	−0.131(2)	0	0.0004(4)	1	0.0290(2)	0.6(6)	180
$\boldsymbol{A}/g_e\beta_e$		−0.0126(2)	0	2	−0.0126(2)	90	270
(mT)			0.0290(2)	3	−0.0131(2)	89.4(6)	0
	−0.0154(3)	0	0.0004(4)	1	0.0278(2)	0.6(6)	0
$\boldsymbol{A}/g_e\beta_e$		−0.0158(2)	0	2	−0.0155(2)	90	180
(mT)			0.0278(2)	3	−0.0158(2)	90	270

[a] Error estimates in parentheses.
[b] Angles θ measures from c-axis and ϕ measured anticlockwise from a-axis.
[c] 32 unit weighted data points, RMSD = 0.0002 mT.
[d] 42 unit weighted data points, RMSD = 0.004 mT.

figure 3. Along with the expected nuclear Zeeman ENDOR lines from ^{91}Zr at 1.441 34 MHz and for ^{29}Si at 3.0104 MHz ($B = 355.60$ mT), there are several important features. There is a nuclear Zeeman ENDOR line at 6.1346 MHz confirming the presence of ^{31}P in the crystal. There is also a pair of strong lines at 5.204 and 7.085 MHz. The spacing between these lines of 1.884 MHz corresponds exactly to the ^{31}P hyperfine interaction observed by EPR. Angular dependence measurements on these lines confirm that these lines are due to ^{31}P hyperfine interaction with the Zr(α) centre. The data from the analysis using EPRNMR given in table 2 agrees well with that from the EPR measurements.

Surrounding the ^{29}Si nuclear Zeeman line are several pairs of lines due to ^{29}Si interaction with the Zr(α) centre (see expanded portion of figure 3). These sets of lines arise from coupling to successive shells of surrounding Si sites. Data from the analysis of the outer pair of these are also given in table 2.

4. Discussion

The combination of the EPR and the ENDOR data show unequivocally that the Zr(α) centre is a complex centre involving a ^{91}Zr nucleus associated with a ^{31}P nucleus. The site splitting observed in the EPR spectra indicates point group symmetry m for the Zr(α) centre, strongly suggesting that both the ^{91}Zr and ^{31}P nuclei lie in the mirror plane. We can now use the analysis of the hyperfine data to determine the site of the ^{31}P in the unit cell and to propose a model for the structure of the centre.

The conclusion reached by Claridge *et al* [3] that most of the spin density resides on the ^{91}Zr atom is confirmed. That most of the unpaired spin is almost entirely in a Zr d-orbital is reflected in the ^{91}Zr hyperfine parameters: following Morton and Preston [13], the unpaired density in the d-orbital is $|b/\alpha P| = |1.313/(\frac{2}{7} \times 5.5525)| = 82.8\%$. In contrast the contribution from the 4s orbital is small: $|a/A| = |6.157/98.22| = 6.3\%$. In this analysis, a and b are the isotropic and anisotropic parts respectively of the experimentally determined hyperfine interaction. A and P are theoretical values taken from [13] for 100% s or p character. α (here $= 2/7$) is the appropriate d-type spherical harmonic contribution to the d orbital. The total unpaired

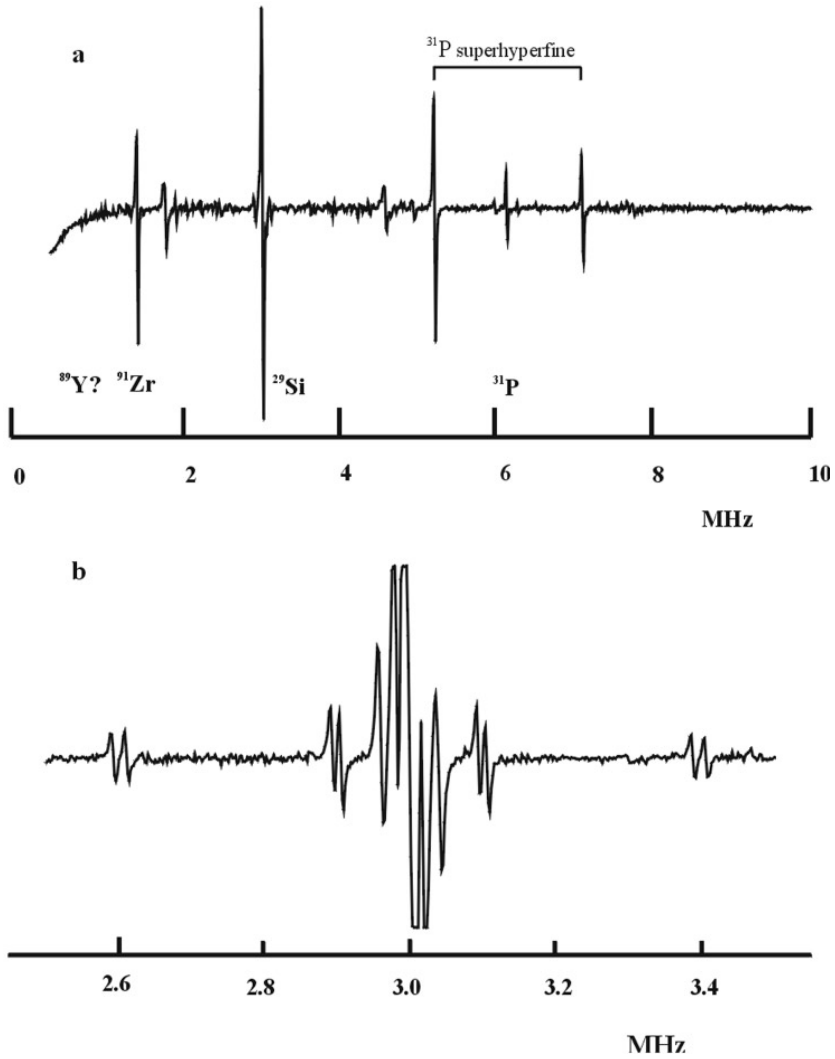

Figure 3. ENDOR spectrum between 0.5 and 10 MHz obtained while saturating on the central lines of the Zr(α) centre. $\boldsymbol{B} = 347.45$ mT, $\nu = 9.344$ GHz. The expanded region shows the multiple ^{29}Si superhyperfine structure.

density on the ^{91}Zr atom is 89.1%. The remaining 10.9% is distributed on the surrounding nuclei.

The above analysis shows that the Zr(α) centre is an electron trap centre; a Zr^{3+} ion at a Zr^{4+} lattice site stabilized by the nearby ^{31}P nucleus. The electronic configuration of Zr^{3+} is $[Kr]4d^1$. The observed g-tensor is almost axially symmetric with $g_\parallel < g_\perp$ (or more precisely $g_{zz} < \frac{1}{2}(g_{xx} - g_{yy})$). Neglecting the lowering of the symmetry caused by the nearby P atom, the lowest d orbital is $|x^2 - y^2\rangle$ under the D_{2d} symmetry of the Zr^{4+} site. Since g_{zz} is almost parallel to the c-axis (deviation from the c-axis of approximately 8°), the $d_{x^2-y^2}$ orbital is almost confined to the ab-plane. The situation is analogous to that of Cr^{3+} in K_3CrO_8, where the $|x^2 - y^2\rangle$ lobes point between the nearby oxygens [14].

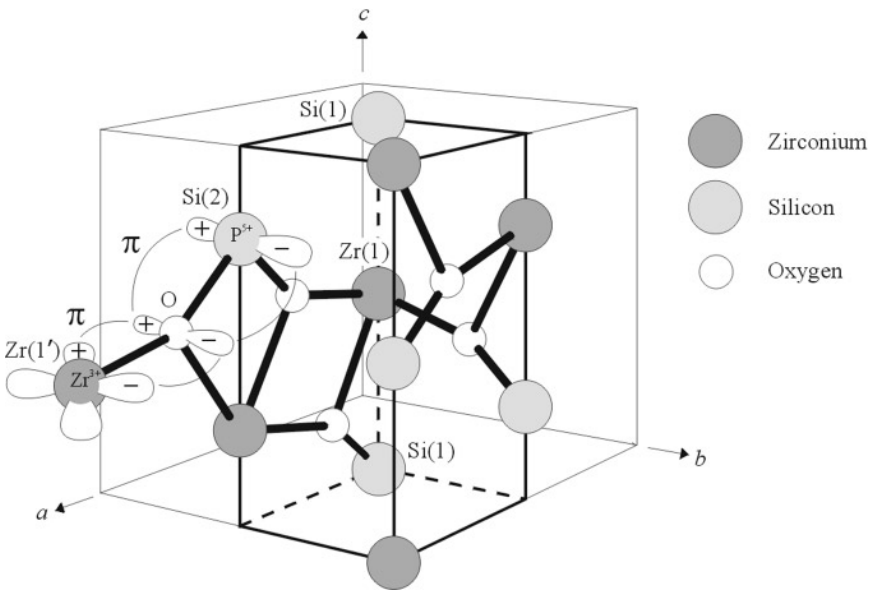

Figure 4. Model illustrating structure of the Zr(α) centre. Note: not all atoms in the unit cell are shown.

The spin density found at the ^{31}P is very small. The 3s contribution is $|a/A| = |0.0383/474.79| = 0.008\%$, and the 3p contribution is $|b/\alpha P| = |0.083/(\frac{2}{5} \times 32.27)| = 0.63\%$. Although small, the interaction between the central Zr^{3+} and the ^{31}P determines the symmetry of the centre. While it is unlikely that a phosphorus will enter a Zr^{4+} site, comparisons of the ionic radii of P^{5+} (35 pm) and Si^{4+} (42 pm) indicate that P^{5+} will easily substitute into a Si^{4+} site forming a stable $[PO_4]^{4+}$ unit. The question of a possible compensating ion will be discussed later.

The observed *m* symmetry requires that the P^{5+} be at the Si(2) site relative to the Zr^{3+} at the Zr(1′) site in figure 4. The Zr(1′) is a site related to Zr(1) by a translation of one unit cell along the *a*-axis. One can exclude an Si(1′) (not shown in figure 4) site for the P, since in this case the largest ^{31}P hyperfine splitting would be along the *c*-axis and the shf tensor would be axially symmetric about the *c*-axis. However, the ^{31}P shf tensor is not axially symmetric; the largest principal value is parallel to the *b*-axis, perpendicular to the Zr(1′)–Si(2) direction. The other two values of the shf tensor lie in the *ac*-plane. The smallest value does not lie along the Zr^{3+}–P^{5+} (Zr(1′)–Si(2)) direction, but is deviated by 2° towards the direction from the Si(2) to the intervening O atom. A classical dipole–dipole calculation, assuming a Zr^{3+}–P^{5+} separation of 362 pm undistorted from the normal Zr^{4+}–Si^{4+} distance in the zircon lattice yields an anisotropic interaction constant of b_{dd}/h of about 0.6 MHz (0.2 mT) in this direction [15]. While this is of the right order of magnitude, the calculation does not yield the largest value in the perpendicular direction. In order to explain the ^{31}P tensor we propose that there is a spin transfer from the Zr^{3+} $d_{x^2-y^2}$ orbital via the intermediate oxygen which is covalently bonded to the P atom. Spin density on the oxygen atom is not observed because of the low abundance (0.038%) of the only magnetic isotope ^{17}O.

The $d_{x^2-y^2}$ overlap with the oxygen 2p orbital along the *b*-direction causes admixture of the oxygen 2p orbital via overlap and possible covalency into the 2s wavefunctions of the unpaired spin density. The oxygen 2p orbital transfers unpaired spin to the ^{31}P 3p orbital via

covalency, thus qualitatively explaining that the largest P shf interaction is along the *b*-axis. Apart from the ^{31}P 2p-orbital mixing, there may be a small P 3s admixture to the small Zr 4s contribution to the wavefunction of the unpaired spin. Note that the unpaired density in the P 3s orbital is three orders of magnitude lower than in the ^{91}Zr 4s orbital. This would be roughly expected if an overlap admixture between the Zr 4s and the O 2s orbital is covalently transferred to the ^{31}P 3s orbital. Of the 6.3% 4s spin density at the Zr about 10^{-3} is found at the ^{31}P. The transfer factor is made up of the square of the overlap integral between the Zr 4s and O 2s orbital and the covalency admixture between the O 2s and P 3s orbitals. Assuming a value of 0.05 for the former and 0.3 for the latter the value of $\sim 10^{-3}$ is obtained. Unfortunately no satisfactory Zr wavefunctions are available to calculate the overlap integrals.

A dipole–dipole mechanism can be assumed for spin density transfer from the Zr^{3+} to the surrounding ^{29}Si atoms. There are three Si atoms occupying (almost) equivalent sites to the ^{31}P at Si(2) relative to the Zr^{3+} at Zr(1′). The ^{29}Si atom which lies on the mirror plane defined by the Zr^{3+}–P^{5+} interaction will be slightly different from the other two at sites perpendicular to this mirror plane. Assuming that the ^{29}Si nuclei will have approximately the same spin density as at the ^{31}P, one can estimate, using the Morton and Preston argument, that there will be an anisotropic shf coupling of 0.025 mT for these ^{29}Si. The expanded section of figure 3 shows that there is interaction with several types of neighbouring silicon atom. The data in table 2 include values for the two largest of these and shows that these are of the order of magnitude expected. The other interactions will be from far more remote silicon sites. In contrast to the ^{31}P tensors the ^{29}Si tensors are almost axially symmetric about the *c*-axis and provide little further information on the centre.

One can speculate as to how the $[PO_4]^{3-}$ unit is stabilized in the $[SiO_4]^{4-}$ site in zircon. The source of the phosphorus is most likely from the molybdate flux from which the crystals are grown. Even very high purity molybdate contains some phosphate which is apparently readily incorporated into the zircon lattice. One might expect that some M^{3+} ion as charge compensator would be needed. This might be Y^{3+}, but, however no evidence of interaction with Y^{3+} at 0.74 MHz was found in the ENDOR spectrum. Although negative, the lack of any form of charge compensator observed by ESR is in line with observations for most other paramagnetic centres in flux grown zircon.

5. Conclusion

Combined high resolution EPR and ENDOR measurements have characterized the principal centre in x-irradiated zircon as an electron centre where the electron is immobilized on a Zr^{4+} atom (to form the Zr^{3+} unit) in the nearest lattice site to a P^{5+} ion substituting for an Si^{4+} ion. The centre can be designated as the $[ZrPO_4]^0$ unit. The centre is seen in all undoped or lightly doped synthetic zircons and in most natural zircons after cold irradiation. Phosphorus present as a very low level impurity in the Li_2MoO_4/MoO_3 melt used to grow the synthetic zircons is evidently very readily incorporated into the zirconium silicate lattice.

Acknowledgments

The authors acknowledge the support from the New Zealand–Federal Republic of Germany Science and Technological Agreement which has made this cooperation possible. Support from the Deutsche Forschungsgemeinschaft and the New Zealand Lotteries Commission is also acknowledged.

References

[1] Hazen R H and Finger L W 1979 *Am. Mineral.* **6** 196–201
[2] Solntsev V P and Shcherbakova M Ya 1973 *Dokl. Akad. Nauk. SSSR* **1** 156–8
[3] Claridge R F C, Mackle K M, Sutton G L A and Tennant W C 1994 *J. Phys.: Condens. Matter* **6** 3429–36
[4] Mombourquette M J, Weil J A and McGavin D G 1996 Computer Program EPRNMR, Department of Chemistry, University of Saskatchewan
[5] Chase A B and Osmer J A 1966 *J. Electrochem. Soc.* **113** 198–9
[6] Claridge R F C, McGavin D G and Tennant W C 1994 *J. Phys.: Condens. Matter* **7** 9049–60
[7] Tennant W C and Claridge R F C 1999 *J. Mag. Reson.* **137** 107–13
[8] Claridge R F C, Mackle K M, Sutton G L A and Tennant W C 1994 *J. Phys.: Condens. Matter* **6** 10 415–22
[9] Claridge R F C, Tennant W C, Schweitzer S and Spaeth J-M 1999 *J. Phys.: Condens. Matter* **11** 8579–89
[10] Weil J A and Anderson J H 1961 *J. Chem. Phys.* **35** 1410–6
[11] Samatov M V, Votyakov S L and Krasnobaev A A 1982 *Izv. Akad. Nauk SSSR, Neorg. Mater.* **18** 1866–8
[12] Krasnobaev A A, Votykov S L and Krochalev V Ya 1988 *Spectroskopya Tsirkonov* (Moscow: Nauka)
[13] Morton J R and Preston K F 1975 *J. Magn. Reson.* **30** 577–82
[14] Swalen J D and Ibers J A 1962 *J. Chem. Phys.* **37** 17–20
[15] Spaeth J-M, Niklas J R and Bartram R H 1992 *Structural Analysis of Point Defects in Solids* (Berlin: Springer)